Structure and Scaling of Helical Modes of Light

Steven Sundbeck and Ilya Gruzberg

The James Franck Institute and Department of Physics, The University of Chicago, Chicago, Illinois 60637

David G. Grier

Department of Physics and Center for Soft Matter Research, New York University, New York, NY 10003

Modes of light containing topological defects such as screw dislocations can be focused into optical traps with interesting and useful properties. This Letter discusses how the intensity distribution within helical modes of light varies with topological charge and introduces new scaling predictions for their radial profiles that are consistent with experimental observations.

OCIS codes: 140.7010, 090.1760, 350.5030

A helical mode of light is characterized by a phase profile, $\varphi(\vec{\rho}) = \ell\theta$, proportional to the angle, θ, about the optical axis. This phase function features a screw dislocation that endows the beam with at least two extraordinary properties. First, the superposition of all phases along the axis results in perfect destructive interference. A helical beam consequently focuses to a dark spot, at least in the paraxial approximation, its intensity being redistributed to a ring of light. The photons in helical beams, furthermore, carry a conserved orbital angular momentum distinct from their intrinsic spin angular momentum.[1] Helical beams thus have potential applications in secure and parallel data communication,[2] with information being carried in topological channels or being encoded in the beam's topology. The orbital angular momentum also can exert useful torques on illuminated objects, particularly when helical beams are focused into ring-like traps known as optical vortices.[3–6] In the decade after their initial demonstration, optical vortices have been used to assemble mesoscopic systems[7] to create microfluidic pumps[8–10] and to establish all-optical atom traps.[11,12]

Many proposed applications take advantage of helical beams' cylindrical intensity distribution. This structure, however, has been the subject of recent debate, with experimental results[9] differing from predictions.[13] Efforts to account for this discrepancy led to the prediction and demonstration of sinusoidally modulated optical vortices.[14] This Letter establishes

both analytically and experimentally that an optical vortex's radius depends linearly on its helicity, ℓ, and introduces scaling functions for helical beams' radial intensity profiles.

Helical beams are readily created from TEM_{00} beams either with conventional mode converters[15,16] or by holographic methods,[3,17,18] with the latter providing a substantially larger range of helicities.[8,9] The resulting field has the general form $E_\ell(\vec{\rho}) = u(\vec{\rho})\exp(i\ell\theta)$, where $\vec{\rho} = (\rho, \theta)$ is the position in a plane normal to the direction of propagation, and $u(\vec{\rho})$ is the real-valued amplitude. The azimuthal index ℓ determines the mode's helicity, and often is referred as the topological charge.

Experiments on helical beams have been interpreted in terms of the properties of Laguerre-Gaussian (LG_p^ℓ) eigenmodes of the Helmholtz equation,[19] which constitute a special case with

$$u_p^\ell(\vec{\rho}) = (-1)^p \left(\sqrt{2}\,\frac{\rho}{w}\right)^\ell L_p^\ell\left(2\,\frac{\rho^2}{w^2}\right) \exp\left(-\frac{\rho^2}{w^2}\right). \tag{1}$$

Here $L_p^\ell(x)$ is a generalized Laguerre polynomial with radial index p, and w is the beam's radius in the observation plane.[1] An LG_p^ℓ mode with $p = 0$ appears as a ring of light with radius $R_\ell = w\sqrt{\ell/2}$.[13] Higher-order LG_p^ℓ modes appear as $p+1$ concentric rings whose radii are more complicated functions of ℓ.

Helical modes with more general radial amplitude profiles can be expressed as superpositions of LG_p^ℓ modes, all with the same azimuthal index ℓ. They would not be expected to share the simple $\sqrt{\ell}$ scaling characteristic of pure $p = 0$ LG_0^ℓ modes. Even less likely is that a superposition of LG_p^ℓ modes would scale *linearly*

$$R_\ell = R_0\left(1 + \frac{\ell}{\ell_0}\right). \tag{2}$$

And yet precisely this result has been obtained experimentally over two orders of magnitude in ℓ.[9] Numerical analysis suggests that linear scaling emerges at least approximately for beams with uniform intensity.[9] Here, we show that this is a far more general result.

Once a beam of light with amplitude profile $u(\vec{\rho})$ is imprinted with a particular phase profile $\varphi(\vec{\rho})$, its propagation into the far field is described by the Fraunhofer diffraction integral,

$$E(r,\psi) = \int_0^\infty d\rho\,\rho\,u(\rho)\int_0^{2\pi} d\theta\, e^{i\varphi(\vec{\rho})}e^{ik\rho\alpha\cos(\theta-\psi)}, \tag{3}$$

where k is the wavenumber of the light, $\vec{r} = (r,\psi)$ are the polar coordinates in the observation plane, and $\alpha = r/z$ at a range $z \gg r$. Equivalently, $\alpha = r/(2f)$ in the focal plane of a lens of focal length f. We will consider Gaussian beams with $u(\rho/a) = \exp(-(\rho/a)^2)$ and "flat top" or pillbox beams with $u(\rho/a) = \Theta(1-\rho/a)$, where $\Theta(x)$ is the Heaviside step function. We introduce the dimensionless radial integration variable $y = \alpha k\rho$ and the rescaled observation coordinate $x = \alpha k a$ and integrate over angles to obtain the transformed helical beam[9,20–22]

$$E_\ell(x,\psi) = 2\pi\, i^\ell\, e^{i\ell\psi}\,\frac{a^2}{x^2}\int_0^\infty dy\, y\, u\left(\frac{y}{x}\right) J_\ell(y), \tag{4}$$

where $J_\ell(y)$ is a Bessel function of order ℓ. For the Gaussian profile, this yields[21]

$$A_\ell(x) = |E_\ell(x,\psi)| = \frac{\pi^{3/2}a^2}{4}\, x e^{-x^2/8}\, \left[I_{\frac{\ell-1}{2}}\left(\frac{x^2}{8}\right) - I_{\frac{\ell+1}{2}}\left(\frac{x^2}{8}\right)\right], \tag{5}$$

where $I_\nu(x)$ is a modified Bessel function of the first kind.

Equation (5) simplifies to a class of scaling solutions for $\ell \gg 1$. This follows from the recursion formula, $I_\nu(\xi) - I_{\nu+1}(\xi) = \left(\frac{\nu}{\xi}+1\right) I_\nu(\xi) - \frac{dI_\nu(\xi)}{d\xi}$, by applying uniform asymptotic expansions for large order (Ref. [23], 9.7.7 and 9.7.9) to obtain

$$I_\nu(\nu\xi) - I_{\nu+1}(\nu\xi) \approx \frac{e^{\nu\eta}}{\sqrt{2\pi\nu}} \frac{1+\xi-(1+\xi^2)^{1/2}}{\xi(1+\xi^2)^{1/4}}. \tag{6}$$

Here, $\eta = \sqrt{1+\xi^2} + \ln\frac{\xi}{1+\sqrt{1+\xi^2}}$. In our case, $\nu = (\ell-1)/2$ and $\nu\xi = x^2/8$ so that $\xi = x^2/[4(\ell-1)]$, and

$$A_\ell(x) \approx \frac{\pi a^2}{4}\frac{x}{\sqrt{2\nu}}\, e^{\nu(\eta-\xi)}\, \frac{1+\xi-(1+\xi^2)^{1/2}}{\xi(1+\xi^2)^{1/4}}, \tag{7}$$

which resembles a similar result in Ref. [21] obtained in a complementary manner.

The ring's intensity peaks for values of x that scale with ℓ. At least near the peak, therefore, and for large ℓ, $\xi \approx \nu \gg 1$. This allows us to approximate the exponent as $\eta - \xi \approx -(2\xi)^{-1} \approx -2\ell/x^2$ and the algebraic term as $\xi^{-3/2} \approx 8\ell^{3/2}/x^3$. In these approximations, the amplitude reduces to

$$A_\ell(x) \approx 2\pi a^2 \frac{\ell}{x^2} e^{-\ell^2/x^2}. \tag{8}$$

The intensity, $\mathcal{I}_\ell(x) = |A_\ell(x)|^2$, thus is peaked at $x = \alpha k a = \ell$, consistent with our assumption, and in agreement with the experimentally observed linear scaling.[9] Equation (8) further suggests that the intensity follows a universal function of x/ℓ

$$\left(\frac{\ell}{2\pi a^2}\right)^2 \mathcal{I}_\ell(x) \approx \left(\frac{\ell}{x}\right)^4 e^{-2(\ell/x)^2}. \tag{9}$$

We tested these predictions by imprinting helical phase profiles onto a Gaussian laser beam and imaging the far-field intensity distribution. Our apparatus is shown schematically in Fig. 1. A collimated TEM_{00} beam from a frequency-doubled diode-pumped Nd:YVO_4 laser operating at $\lambda = 532$ nm (Coherent Verdi) was attenuated and polarized by passing through a half-wave plate and polarization-selective beam splitter before being spatially filtered with a Keplerian beam expander. The resulting collimated beam has a Gaussian profile with half-width $w = 8$ mm, and substantially fills the 20 mm diagonal face of a Holoeye LC2002 twisted-nematic liquid crystal spatial light modulator (SLM). This SLM imposes phase shifts over the range 0 to 2π radians at each 20 μm wide pixel in an 800×600 array. Nearly phase-only modulation was achieved by placing a half-wave plate before the SLM and an analyzer after. The resulting discrete approximation to a helical beam was projected by a lens of

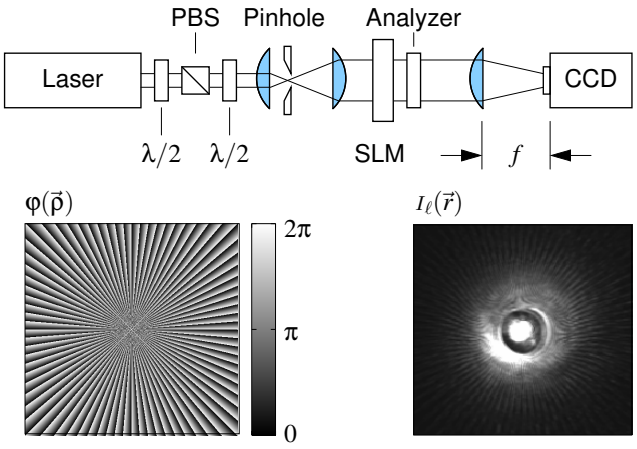

Fig. 1. Optical train used to image helical modes together with a typical phase mask, $\varphi(\vec{\rho}) = \ell\theta \bmod 2\pi$, with $\ell = 80$, and the resulting intensity $\mathcal{I}_\ell(\vec{r})$. The central spot results from the undiffracted portion of the beam.

focal length $f = 300$ mm onto the 2/3 inch diagonal face of a monochrome CCD camera. The measured intensity pattern should be well described by scalar diffraction theory. This need not have been the case in previous studies,[9,14] which employed high-numerical aperture optics. A typical far-field intensity pattern with $\ell = 80$ appears in Fig. 1. As in previous studies,[8,9,21] diffraction by the SLM's pixels creates ℓ radial striations, which do not affect the measured radii.

Figure 2(a) shows radial intensity profiles obtained by averaging digitized images over angles around the optical axis for helical modes with topological charges ranging from $\ell = 50$ to $\ell = 300$. As Eq. (9) predicts, the principal maximum broadens and moves to larger radius with increasing topological charge. The peak intensity falls off as ℓ increases because the same amount of light is distributed over a larger area. Rescaling according to Eq. (9) does not collapse the data particularly well. Instead, the excellent collapse shown in Fig. 2(b) is obtained by offsetting ℓ by an empirically determined factor, $\ell_0 = 21$. The resulting profiles indeed collapse onto a universal scaling function peaked at $x = \alpha\kappa a = \ell - \ell_0$. Adjusting ℓ_0 to minimize the mean-square deviations yields good agreement in both the peak height and position, with agreement improving for larger ℓ.

Were linear scaling specific to Gaussian profiles, it would be a curiosity. However, it arises in other cases of practical interest. For example, the far-field amplitude for a helically-modulated pill-box beam is

$$A_\ell(x) = \frac{2\pi a^2}{x^2} \int_0^x J_\ell(y)\, y\, dy \tag{10}$$

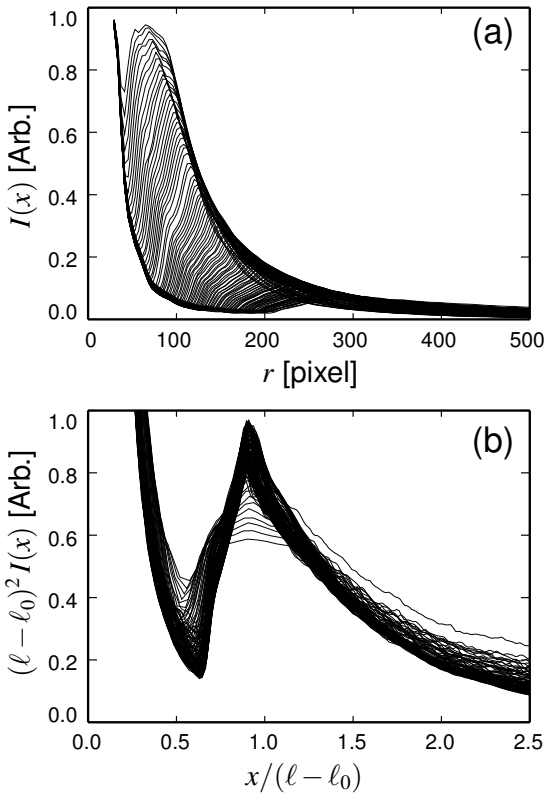

Fig. 2. Scaling of the radial intensity profile with topological charge. (a) Azimuthally averaged intensity profiles for helical modes with topological charges ranging from $\ell = 50$ to $\ell = 300$. Both the peak height and radius vary with ℓ. (b) Rescaled profiles collapse onto a single master curve.

The principal maximum occurs when x reaches $j_{\ell,1}$, the first zero of $J_\ell(y)$, which scales as $j_{\ell,1} \approx \ell + 1.856\,\ell^{1/3}$ for $\ell \gg 1$.[23] Thus the ring's radius again scales roughly linearly with ℓ. Obtaining linear scaling for both the Gaussian and flat-top profiles emphasizes this surprising result's generality. This is all the more striking because the associated scaling form for the intensity profile, $\ell\, A_\ell(x) \approx 2\pi a^2 \int_{-\xi}^{\infty} \mathrm{Ai}(y)\, dy$, where $x = \ell + (\ell/2)^{1/3}\,\xi$ and $\mathrm{Ai}(x)$ is the Airy function, differs substantially from that for the Gaussian helical beam. The origin of the experimentally observed offset, ℓ_0, however, remains unresolved.

This work was supported by the MRSEC program of the NSF under Grant Number DMR-0213745 and by NSF Grant Number DMR-0304906.

References

1. L. Allen, M. W. Beijersbergen, R. J. C. Spreeuw, and J. P. Woerdman, "Orbital angular-momentum of light and the transformation of Laguerre-Gaussian laser modes," Phys.

Rev. A **45,** 8185–8189 (1992).

2. J. Leach, M. J. Padgett, S. M. Barnett, S. Franke-Arnold, and J. Courtial, "Measuring the orbital angular momentum of a single photon," Phys. Rev. Lett. **88,** 257901 (2002).
3. H. He, N. R. Heckenberg, and H. Rubinsztein-Dunlop, "Optical particle trapping with higher-order doughnut beams produced using high efficiency computer generated holograms," J. Mod. Opt. **42,** 217–223 (1995).
4. H. He, M. E. J. Friese, N. R. Heckenberg, and H. Rubinsztein-Dunlop, "Direct observation of transfer of angular momentum to absorptive particles from a laser beam with a phase singularity," Phys. Rev. Lett. **75,** 826–829 (1995).
5. K. T. Gahagan and G. A. Swartzlander, "Optical vortex trapping of particles," Opt. Lett. **21,** 827–829 (1996).
6. N. B. Simpson, L. Allen, and M. J. Padgett, "Optical tweezers and optical spanners with Laguerre-Gaussian modes," J. Mod. Opt. **43,** 2485–2491 (1996).
7. M. P. MacDonald, L. Paterson, K. Volke-Sepulveda, J. Arlt, W. Sibbett, and K. Dholakia, "Creation and manipulation of three-dimensional optically trapped structures," Science **296,** 1101–1103 (2002).
   three-dimensional trapping pattern.
8. J. E. Curtis, B. A. Koss, and D. G. Grier, "Dynamic holographic optical tweezers," Opt. Comm. **207,** 169–175 (2002).
9. J. E. Curtis and D. G. Grier, "Structure of optical vortices," Phys. Rev. Lett. **90,** 133901 (2003).
10. K. Ladavac, K. Kasza, and D. G. Grier, "Sorting by periodic potential energy landscapes: Optical fractionation," Phys. Rev. E **70,** 010901(R) (2004).
11. T. Kuga, Y. Torii, N. Shiokawa, and T. Hirano, "Novel optical trap of atoms with a doughnut beam," Phys. Rev. Lett. **78,** 4713–4716 (1997).
12. D. McGloin, G. C. Spalding, H. Melville, W. Sibbet, and K. Dholakia, "Applications of spatial light modulators in atom optics," Opt. Express **11,** 158–166 (2003).
13. M. J. Padgett and L. Allen, "The Poynting vector in Laguerre-Gaussian laser modes," Opt. Comm. **121,** 36–40 (1995).
14. J. E. Curtis and D. G. Grier, "Modulated optical vortices," Opt. Lett. **28,** 872–874 (2003).
15. M. W. Beijersbergen, L. Allen, H. E. L. O. van der Veen, and J. P. Woerdman, "Astigmatic laser mode converters and transfer of orbital angular-momentum," Opt. Comm. **96,** 123–312 (1993).
16. R. M. Jenkins, J. Benerji, and A. R. Davies, "The generation of optical vortices and shape preserving vortex arrays in hollow multimode waveguides," J. Opt. A **3,** 527–532 (2001).

17. N. R. Heckenberg, R. McDuff, C. P. Smith, H. Rubinsztein-Dunlop, and M. J. Wegener, "Laser beams with phase singularities," Opt. Quantum Elect. **24,** S951–S962 (1992).
18. J. Arlt, K. Dholakia, L. Allen, and M. J. Padgett, "The production of multiringed Laguerre-Gaussian modes by computer-generated holograms," J. Mod. Opt. **45,** 1231–1237 (1998).
19. A. E. Siegman, *Lasers* (University Science Books, Sausalito, CA, 1986).
20. M. S. Soskin, V. N. Gorshkov, M. V. Vasnetsov, J. T. Malos, and N. R. Heckenberg, "Topological charge and angular momentum of light beams carrying optical vortices," Phys. Rev. A **56,** 4064–4075 (1997).
21. Z. S. Sacks, D. Rozas, and G. A. Swartzlander, "Holographic formation of optical-vortex filaments," J. Opt. Soc. Am. B **15,** 2226–2234 (1998).
22. M. V. Berry, "Optical vortices evolving from helicoidal integer and fractional phase steps," J. Opt. A **6,** 259–269 (2004).
23. M. Abramowitz and I. A. Stegun, *Handbook of mathematical functions* (United States Department of Commerce, Washington, D.C., 1972).